

Lung-Derived SOD3 Attenuates Neurovascular Injury After Transient Global Cerebral Ischemia

Nguyen Mai, PhD; Kathleen Miller-Rhodes, MS; Viollandi Prifti, BS; Minsoo Kim, PhD; Michael A. O'Reilly, PhD; Marc W. Halterman, MD, PhD

Background—Systemic innate immune priming is a recognized sequela of post-ischemic neuroinflammation and contributor to delayed neurodegeneration. Given mounting evidence linking acute stroke with reactive lung inflammation, we asked whether enhanced expression of the endogenous antioxidant extracellular superoxide dismutase 3 (SOD3) produced by alveolar type II pneumocytes would protect the lung from transient global cerebral ischemia and the brain from the delayed effects of ischemia-reperfusion.

Methods and Results—Following 15 minutes of global cerebral ischemia or sham conditions, transgenic SOD3 and wild-type mice were followed daily for changes in weight, core temperature, and neurological function. Three days after reperfusion, arterial and venous samples were collected for complete blood counts, flow cytometry, and SOD3 protein blotting, and immunohistochemistry was performed on lung and brain tissue to assess tissue injury, blood-brain barrier permeability, and neutrophil transmigration. Relative to ischemic controls, transgenic SOD3 mice performed better on functional testing and exhibited reduced peripheral neutrophil activation, lung inflammation, and blood-brain barrier leak. Once released from the lung, SOD3 was predominantly not cell associated and depleted in the venous phase of circulation.

Conclusions—In addition to reducing the local inflammatory response to cerebral ischemia, targeted enrichment of SOD3 within the lung confers distal neuroprotection against ischemia-reperfusion injury. These data suggest that therapies geared toward enhancing adaptive lung-neurovascular coupling may improve outcomes following acute stroke and cardiac arrest. (*J Am Heart Assoc.* 2019;8:e011801. DOI: 10.1161/JAHA.118.011801.)

Key Words: blood-brain barrier • global ischemia • inflammation • lung

Acute central nervous system ischemia triggers the release of damage-associated molecular patterns, initiating a cascade of inflammatory responses in the periphery, including the activation and recruitment of polymorphonuclear neutrophils (PMNs) into postischemic tissues. Peripheral innate immune priming has been implicated in a range of other noninfectious models of acute organ injury involving the

kidney, lung, and liver. And while global PMN activation correlates with poor outcomes after stroke and cardiac arrest,^{1–3} therapeutic trials targeting innate immune responses following stroke or cardiac arrest have been unsuccessful.^{4–6}

The association between brain ischemia and reactive lung inflammation has been described recently.^{7–9} In addition to being the primary vascular bed receiving systemic lymphatic return, the lung filters blood at a rate of 5 L/min, making contact with 10⁹/L leukocytes on average.¹⁰ Consequently, the lung is well positioned to moderate systemic innate immune responses by either removing primed immune cells from circulation¹¹ or influencing their activation. PMNs migrate from remote sites of tissue damage to the lung, where they provoke pulmonary edema and inflammation.¹² Summers and colleagues¹³ studied transpulmonary leukocyte migration and found that exogenously primed PMNs were preferentially retained in the lung relative to unprimed PMNs. Importantly, PMN priming has been shown to be reversible,¹⁴ and under conditions of low-grade systemic inflammation, the pulmonary endothelium appears to play a role.¹⁵ To this point, Nahum et al¹⁶ compared PMN H₂O₂ production between

From the Departments of Neurology (M.W.H.), Neuroscience (N.M., K.M.-R., M.W.H.), Microbiology & Immunology (M.K.), and Pediatrics (M.A.O., M.W.H.), and the Center for Neurotherapeutics Discovery (N.M., K.M.-R., V.P., M.W.H.), School of Medicine and Dentistry, The University of Rochester, NY.

Accompanying Tables S1 through S3 are available at <https://www.ahajournals.org/doi/suppl/10.1161/JAHA.118.011801>

Correspondence to: Marc W. Halterman, MD, PhD, Center for Neurotherapeutics Discovery, Box 645, University of Rochester Medical Center, 601 Elmwood Avenue, Rochester, NY 14642. E-mail: marc_halterman@urmc.rochester.edu
Received December 17, 2018; accepted March 28, 2019.

© 2019 The Authors. Published on behalf of the American Heart Association, Inc., by Wiley. This is an open access article under the terms of the Creative Commons Attribution-NonCommercial License, which permits use, distribution and reproduction in any medium, provided the original work is properly cited and is not used for commercial purposes.

Clinical Perspective

What Is New?

- In addition to priming peripheral innate immunity, cerebral ischemia induces reactive inflammatory changes within the lung.
- Enhanced expression of superoxide dismutase 3 within the lung reverses both systemic and lung inflammatory markers.
- Superoxide dismutase 3 produced and shed by the lung reduces cerebrovascular injury and behavioral deficits associated with transient global ischemia.

What Are the Clinical Implications?

- These findings implicate lung-neurovascular coupling as a critical component in the pathological response to acute cerebral ischemia.
- Given its position in the cardiovascular system and importance in postischemic systemic immune priming, these studies also frame the lung as a tractable target for therapeutic intervention after acute ischemic stroke and cardiac arrest.

venous and arterial blood and found patients with increased arterial production with acute respiratory distress syndrome compared with control subjects. Thus, beyond its role in moderating gas exchange, these data suggest that the lung may moderate systemic inflammatory responses to tissue ischemia and secondary injury during reperfusion.

Extracellular superoxide dismutase 3 (SOD3) expressed primarily in the lung and kidney is the major antioxidant within the vascular extracellular space and is essential for survival in the presence of ambient oxygen.^{17,18} Global expression of SOD3 under the ubiquitous *Actb* promoter protects the brain against both hypoxic and hyperoxic stress.^{19,20} However, selective expression of human SOD3 (hSOD3) in type II alveolar epithelial cells is alone sufficient to protect mice from normobaric, hyperoxic lung through both redox and immune-mediated mechanisms.^{21,22} Given these observations, we asked whether the focal manipulation of lung inflammation through the enforced expression of hSOD3 would likewise reduce both postischemic peripheral immune priming and neurovascular injury.³

Materials and Methods

Global Cerebral Ischemia Model

The data that support the findings of this study are available from the corresponding author upon reasonable request. This article adheres to the AHA's implementation of the Transparency and Openness Promotion Guidelines. All experimental

protocols were approved by the University of Rochester Committee on Animal Resources. hSOD3 was expressed under the surfactant protein-C promoter as described.²² Six- to 8-week-old wild-type (WT) and transgenic superoxide dismutase 3 (TgSOD3) C57BL/6 male mice (25–30 g) were numbered and randomized by the QuickCalcs subjects randomizer (GraphPad, La Jolla, CA) into sham and 3-vessel occlusion (3VO) groups (Figure 1A). On day –10, all mice underwent basilar artery occlusion.²³ Surgical anesthesia was induced using a single intraperitoneal dose of ketamine/ xylazine (100 mg/kg, 10 mg/kg). On day 0, the 3VO group underwent transient bilateral common carotid artery occlusion (15 minutes), with controls undergoing neck dissection without occlusion. Mice were excluded if cerebral blood flow by laser Doppler flowmetry (Perimed, Ardmere, PA) did not fall below 75% of control values during bilateral common carotid artery occlusion (Figure 1B). Daily weights and rectal temperatures were recorded (Figure 1C and 1D). WT and TgSOD3 group sizes after Doppler exclusion were as follows: sham (n=4) and 3VO (n=7). Sample size calculations were based on mean differences in neurological function score between 3VO-treated WT (9.3±1.2) and TgSOD3 mice (11.6±0.9) observed in our pilot work (n=3 for $\alpha=0.05$ /power=0.8). Additional animals were allocated to each arm to account for possible mortality, though no animals died before the conclusion of the experiment, and all were used in data analyses. The data presented represent the results of a single trial.

Analyses of Neurological Function

Global neurological function was assessed using a composite scoring system used to assess mice after global brain ischemia-reperfusion (Table S1). Domains assessed include level of consciousness, spontaneous movement, gait, touch escape response, corneal reflex, and respiration.⁹ Assessments were performed on days –10 (before basilar artery occlusion), 0 (before bilateral common carotid artery occlusion/sham), 1, and 3. Investigators involved in the behavioral assessments were blinded to group allocation during both data collection and analysis.

Immunohistochemistry and Image Analyses

Following intracardiac perfusion and inflation fixation of the lungs, tissues were removed, postfixed in 4% paraformaldehyde (Sigma-Aldrich, St Louis, MO), cut into 25- μ m sections using a Leica SM2010R microtome (Leica Biosystems, Buffalo Grove, IL), and stored at 4°C in cryoprotectant. Sections were washed with phosphate-buffered saline and blocked in 10% goat serum for 1 hour at 20°C prior to immunohistochemical staining using antibodies as listed in Table S2. Investigators were blinded to sample assignments by using an

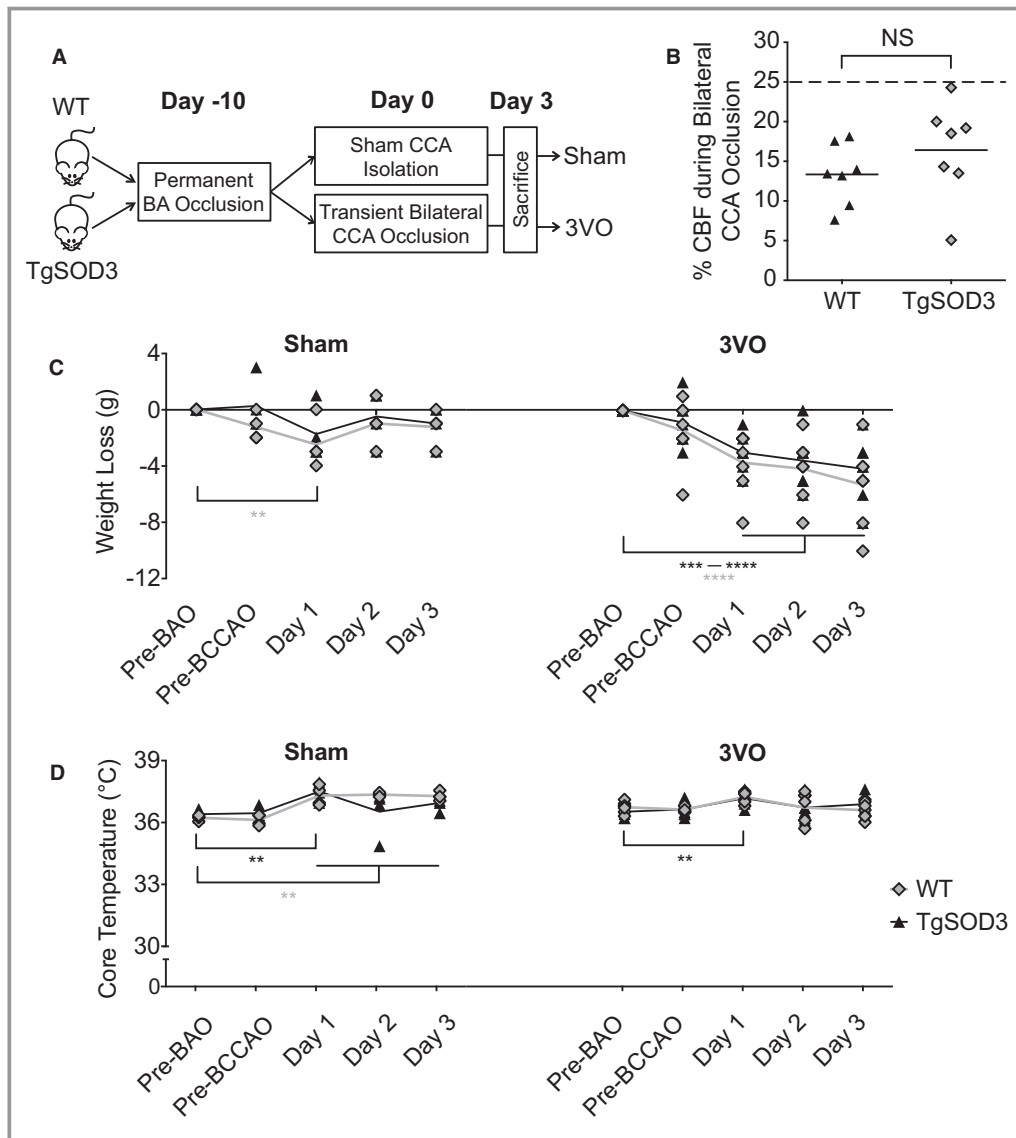


Figure 1. Study design and physiological parameters. **A**, Adult male WT and TgSOD3 mice were randomly assigned to sham and 3-vessel occlusion (3VO) treatment groups. Ten days following permanent basilar artery (BA) occlusion, animals underwent either sham surgery or bilateral common carotid artery (CCA) occlusion for 15 minutes. Animals were euthanized after 3 days. **B**, During CCA occlusion, cerebral blood flow (CBF) fell below 25% of pretreatment values with no difference between WT and TgSOD3 mice ($n=7$; unpaired 2-tailed t test: $P=0.29$). **C**, Changes in weight caused by surgical manipulation. Values represent means \pm SD ($n=4-7$). Repeated measures ANOVA with the Holm-Sidak post hoc test: ** $P<0.01$, *** $P<0.001$, **** $P<0.0001$ compared with pre-basilar artery occlusion (BAO) values. BCCAO indicates bilateral common carotid artery occlusion; TgSOD3, transgenic superoxide dismutase 3; WT, wild type.

alphanumeric coding strategy. Sections were imaged using an OptiGrid Structured-Light Imaging System (Qioptiq, Fairport, NY). Cortical Ly-6B(+) PMN counts and percent injury calculations based on regional loss of microtubule-associated protein 2 staining were calculated from images taken at $\times 10$ magnification from 5 to 8 matched, noncontiguous coronal sections spanning +1.70 to -2.92 mm from bregma. Iba1 upregulation, platelet endothelial cell adhesion molecule

upregulation, and immunoglobulin G leakage were measured by mean gray values (fluorescence intensity) from 4 random cortical sections imaged at $\times 20$ magnification per mouse. Immunoglobulin G intensity was normalized to platelet endothelial cell adhesion molecule (+) vessel length. Lung PMN infiltration was estimated by measurement of Ly-6B mean gray value in 10 random sections, and cellularity was measured by counting Hoechst-labeled nuclei in 5

compressed Z-stack images per animal. Alveolar wall thickness was measured as the smallest orthogonal distance between 2 adjacent alveoli. Images for lung quantifications were acquired at $\times 40$ magnification. Images were acquired using identical settings and values to minimize variability and analyzed using ImageJ (<http://rsb.info.nih.gov/ij/>). Micrographs were pseudocolored after analyses for consistency.

Analyses of SOD3 Expression in Arterial and Venous Blood

Western blotting was performed on brain, lung, spleen, kidney, and liver homogenates as well as arterial (aorta) and venous (retro-orbital sinus), and the cell fraction from these blood samples were lysed in radioimmunoprecipitation assay buffer. Blots were probed with antibodies as indicated in Table S2 and imaged using the Azure c600 (Azure Biosystems, Dublin, CA). The data presented represent the results of a single trial.

Flow Cytometry and Complete Blood Counts

Analyses were performed on retro-orbital blood collected at 2 hours after experimental treatment. Whole blood was washed and incubated with red cell lysis buffer (Biolegend, San Diego, CA) for 5 minutes at 4°C. White blood cells were stained with fluorescein isothiocyanate–labeled anti-Ly-6G (1 $\mu\text{g}/\text{mL}$; 30 minutes, 4°C) and Alexa Fluor 647-labeled anti-CD11b antibodies (0.8 $\mu\text{g}/\text{mL}$) (BioLegend). Cells were later fixed in 2% paraformaldehyde for 30 minutes, and fluorescence was measured using a BD FACSCanto II Flow Cytometer (BD Biosciences, San Jose, CA). Data were collected from 10 000 events, and PMNs were identified on the basis of scatter and expression of Ly-6G (clone 1A8) and CD11b. In a separate cohort, retro-orbital blood was collected 6 hours after experimental treatment for complete blood count using a Vetscan HM5 blood analyzer (Abaxis, Union City, CA). The data presented represent the results of a single trial.

Statistical Analyses

Statistical analyses were performed using Prism 6 (GraphPad, La Jolla, CA). Data are expressed as the average \pm standard deviation. Data sets from all experiments were assessed for normality with the Shapiro–Wilk test (Table S3). Physiological parameters and neurological function score were analyzed by repeated measures ANOVA with the Holm-Sidak post hoc test. Cortical injury, cortical PMN infiltration, platelet endothelial cell adhesion molecule expression, immunoglobulin G leakage, lung PMN infiltration, lung cellularity, and alveolar wall thickness were analyzed by 2-way ANOVA (treatment

group versus genotype) with the Holm-Sidak post hoc test. Data sets with a nonnormal distribution (lung PMN infiltration and alveolar wall thickness) were analyzed by 2-way ANOVA with the Holm-Sidak post hoc test following natural log transformation. Results of the back-transformed data are presented in text, with histograms (Figure 2) showing raw data points and back-transformed means with associated 95% confidence intervals. Cerebral blood flow changes between WT and TgSOD3 mice were analyzed using an unpaired 2-tailed t test. For flow cytometry experiments, geometric mean fluorescence intensities (MFI) were calculated using FlowJo analysis software (TreeStar, Ashland, OR). Comparisons were made using 2-way ANOVA (vascular source versus genotype) and the Holm-Sidak post hoc test for analyses of densitometric data from human and mouse SOD3 Western blots. $P < 0.05$ were considered significant.

Results

Global Cerebral Ischemia induces Lung Inflammation and Edema

Acute brain injury induces inflammation and edema within the lung.⁸ The extent to which transient global ischemia induces acute lung injury and, consequently, how acute lung injury influences cerebral ischemia-reperfusion injury remains unexplored. Here, we asked whether targeted expression of hSOD3 within type II pneumocytes would protect mice against global cerebral ischemia (Figure 1A). We confirmed the expected reduction in cerebral blood flow after the 3VO procedure using laser Doppler flowmetry and confirmed equivalency between genotypes (WT, $13.3 \pm 3.9\%$ versus TgSOD3, $16.4 \pm 6.2\%$; $P = 0.29$) ruling out potential confounding effects of SOD3 expression (Figure 1B). Relative to sham controls, the 3VO procedure caused progressive weight loss from day -10 to day 3 in both WT (-2.9 ± 1.0 g, $P < 0.0001$) and TgSOD3 mice (-2.3 ± 0.8 g; $P = 0.0001$) (Figure 1C). Despite minor fluctuations, core body temperature remained between 36°C and 38°C in both the 3VO and sham groups (Figure 1D).

Western analyses confirmed that the surfactant protein-C promoter confined human SOD3 expression to the lung while endogenous mouse SOD3 was detected in both the lung and kidney (Figure 2A). Notably, neither human nor mouse SOD3 were expressed to any appreciable degree in whole brain lysates. We next tested whether transient global ischemia induced acute lung injury and whether TgSOD3 expression within the lung reversed this phenotype. Results show that the 3VO procedure induced a robust inflammatory response in the WT lung characterized by the accumulation of Ly-6B(+) PMNs (63.1 [95% CI, 53.5–74.3] versus sham, 36.2 [95% CI, 27.8–47.0]; $P = 0.0019$), increased cellularity of the lung

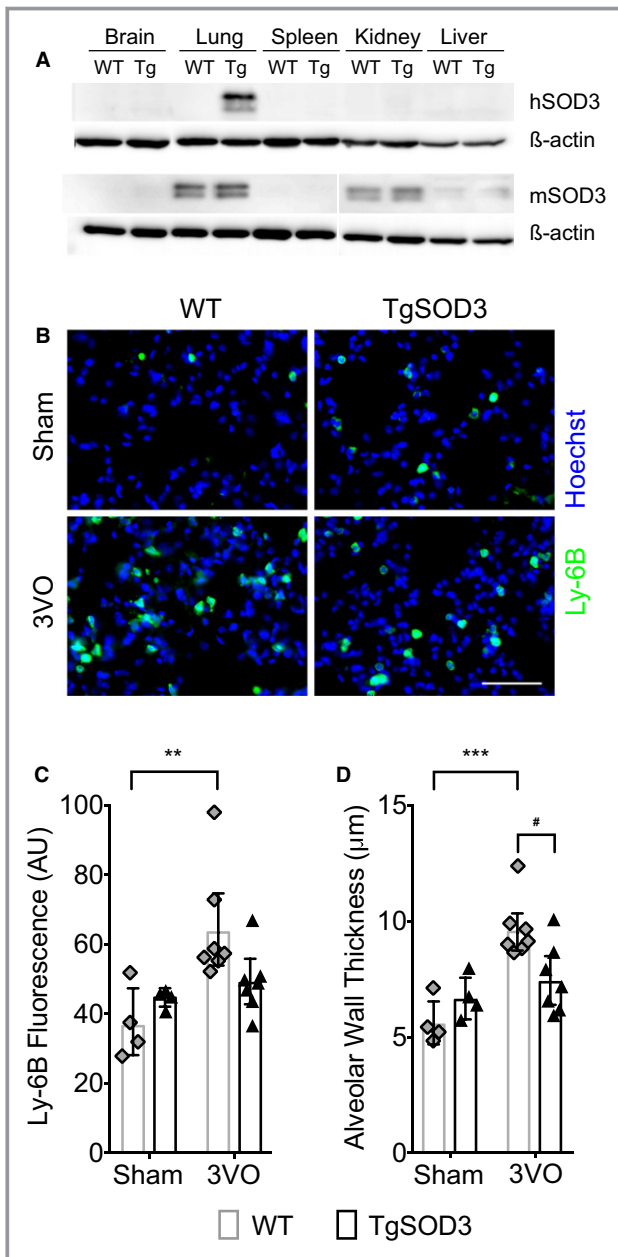


Figure 2. Targeted expression of hSOD3 protects against ischemia-induced acute lung injury. **A**, Western blot showing basal expression of hSOD3 and mouse SOD3 in somatic tissues isolated from wild-type (WT) and TgSOD3 mice. **B**, Lung immunohistochemical demonstrating the effects of 3-vessel occlusion (3VO) on Ly-6B(+) PMN infiltration (green) and overall cellularity (Hoechst-labeled nuclei, blue). Scale bar=50 μm. **C** and **D**, Quantification of PMN accumulation (Ly-6B fluorescence) and alveolar wall thickness in the lung. Raw data points are presented with histograms showing back-transformed means (n=4–7). Error bars span 95% confidence intervals. 2-way ANOVA with the Holm-Sidak post hoc test of natural log-transformed data: Values represent means±SD (n=4–7). ** $P<0.01$, *** $P<0.001$ between sham and 3VO; # $P<0.05$ between WT and TgSOD3. hSOD3 indicates human superoxide dismutase 3; PMN, polymorphonuclear neutrophil; SOD3, superoxide dismutase 3; TgSOD3, transgenic superoxide dismutase 3.

parenchyma ($9.9 \times 10^5 \pm 2.3 \times 10^5$ nuclei/cm² versus sham, $7.2 \times 10^5 \pm 0.5 \times 10^5$ nuclei/cm²; $P=0.047$), and edema within the alveolar wall (9.5 μm [95% CI, 8.7–10.3 μm] versus Sham, 5.5 μm [95% CI, 4.7–6.5 μm]; $P=0.0002$). Conversely, lung tissue from TgSOD3 mice was resistant to 3VO-induced septal thickening (7.3 μm [95% CI, 6.4–8.5 μm] versus sham, 6.6 μm [95% CI, 5.7–7.5 μm]; $P=0.28$) and remained less congested compared with WT lungs ($P=0.026$) (Figure 2B and 2D). These results indicate that global cerebral ischemia induces lung injury and inflammation, which can be attenuated by targeted expression of SOD3 within the lung.

Targeted Expression of hSOD3 in the Lung Limits Peripheral PMN Activation

We next investigated whether targeted hSOD3 within the lungs of TgSOD3 mice would influence postischemic peripheral neutrophil activation. Complete blood counts in WT and TgSOD3 mice 6 hours following sham and 3VO conditions revealed no significant changes with respect to either genotype or surgical intervention (Figure 3A). Flow cytometric analyses performed on the WT background revealed increased CD11b expression on circulating Ly-6G^{hi}/CD11b^{hi} PMNs 2 hours after 3VO (MFI^{sham}: 16 684 versus MFI^{3VO}: 25 826). Conversely, CD11b expression on PMNs from TgSOD3 mice remained stable (MFI^{sham}: 15,044 versus MFI^{3VO}: 14,928) (Figure 3B). These indicate that transient global ischemia is sufficient to induce peripheral PMN activation without increasing the circulating PMN pool, and targeted SOD3 in the lung blocks this response.

Lung SOD3 Prevents Functional Decline and Neurovascular Damage

Using a multiparametric assessment of neurological function, we found that the 3VO procedure induced functional decline in WT mice (9.3 ± 1.2 versus sham, 12.0 ± 0.0 ; $P=0.0006$), while TgSOD3 mice were protected against this stress (3VO, 11.6 ± 1.0 versus sham, 12.0 ± 0.0 ; $P=0.90$) (Figure 4). Using loss of microtubule-associated protein 2 signal and PMN infiltration as surrogates for parenchymal damage, we performed immunohistochemical to correlate these behavioral changes with neuronal injury. Quantitative immunohistochemical analyses measured on day 3 confirmed a net increase in the extent of 3VO-induced damage in WT mice ($28.2 \pm 11.3\%$ versus sham, $8.6 \pm 2.0\%$; $P=0.009$). While there was a trend toward reduced injury, the effect in TgSOD3 mice did not reach significance (3VO, $21.3 \pm 8.9\%$ versus sham, $8.7 \pm 1.7\%$; $P=0.10$). Similarly, comparisons between 3VO and sham groups by 2-way ANOVA revealed a significant treatment effect on cortical PMN infiltration [$F(1,18)=9.045$; $P=0.008$], genotype differences were not observed.

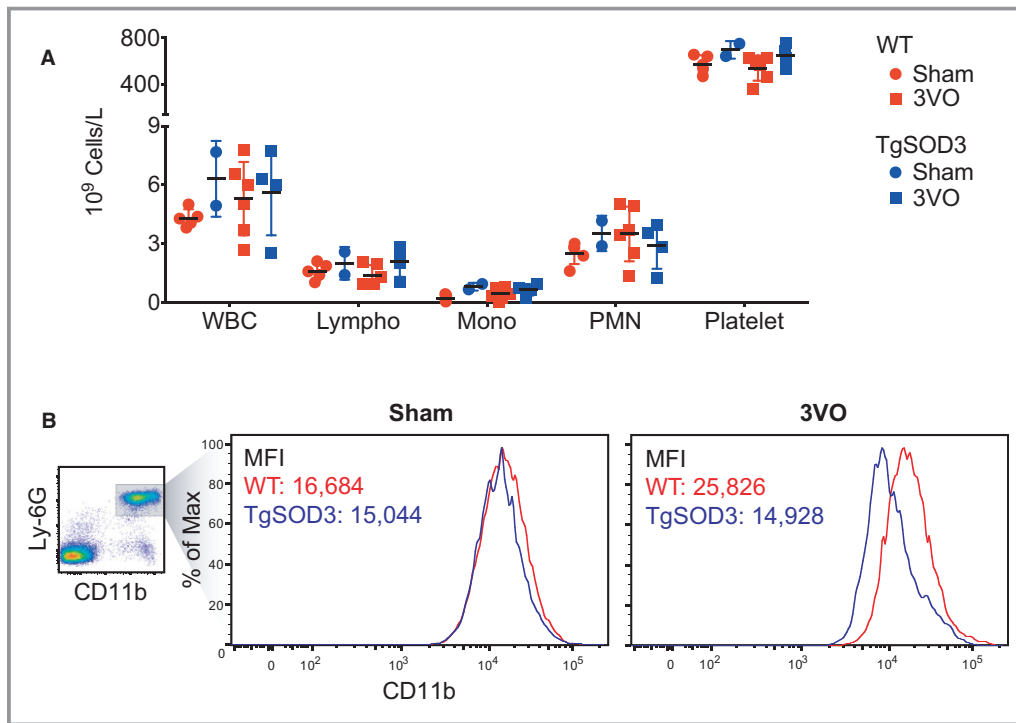


Figure 3. Lung SOD3 reduces neutrophil priming after transient global ischemia. **A**, Complete blood counts including white blood cell (WBC), lymphocyte (lympho), monocyte (Mono), neutrophil (PMN) and platelet counts from WT and TgSOD3 mice 6 hours following the sham and 3-vessel occlusion (3VO) procedures. Values represent the mean \pm SD (n=2–6) for 2-way ANOVA with the Holm-Sidak post hoc test. **B**, Gating strategy used to identify CD11b expression levels on Ly-6G neutrophils isolated from the peripheral circulation and mean fluorescence intensity (MFI) results. Surface CD11b levels on Ly-6G^{hi}/CD11b^{hi} neutrophils were measured 2 hours following either sham or 3VO procedures, which show the depriving effects of SOD3 on ischemia-exposed PMNs. PMN indicates polymorphonuclear neutrophil; SOD3, superoxide dismutase 3; TgSOD3, transgenic superoxide dismutase 3.

Lung SOD3 is Shed to the Systemic Circulation

We next asked whether SOD3 expression could impart cerebrovascular protection in the face of ischemia-reperfusion injury. Immunohistochemical analyses revealed that, while 3VO-induced ischemia did not alter the expression of platelet endothelial cell adhesion molecule-1 in cortical vessels (data not shown), it triggered blood-brain barrier permeability in WT mice (7.5 ± 4.8 versus sham, 1.8 ± 0.4 ; $P=0.033$) reflected by the extravasation of serum immunoglobulin G from the vessel lumen into the parenchyma (Figure 5A and 5B). Notably, SOD3 conferred protection against ischemia-induced blood-brain barrier leak within (Tg/3VO 3.0 ± 0.6 versus Tg/sham 2.2 ± 0.7 ; $P=0.88$) and between genotypes (WT/3VO versus Tg/3VO; $P=0.045$). While SOD3-dependent neurovascular protection could reflect reduced systemic innate immune activation, we asked whether free SOD3 released from the lung might have direct effects on the distal vasculature. Western analyses on whole blood revealed that the majority of SOD3 was localized to the cell-free fraction of arterial specimens in both TgSOD3 (2.3 ± 0.7 versus 0.1 ± 0.0 ;

$P=0.001$) and WT mice (1.6 ± 1.0 versus 0.1 ± 0.0 ; $P=0.002$). Analyses of the cellular fraction from whole blood (WBC+RBC) revealed similar enrichment of both human [$F(1,8)=8.761$; $P=0.018$] and murine [$F(1,8)=44.98$; $P=0.0002$] SOD3 in arterial samples. These results suggest that SOD3 produced by the lung could moderate cerebral reperfusion injury by reducing leukocyte activation during transit and by directly stabilizing the distal cerebral arterial endothelium.

Discussion

Global overexpression of SOD3 driven by the ubiquitous *Actb* promoter protects against both hypoxic and hyperoxic brain injury.^{19,20} However, this model does not accurately reflect the nuanced in vivo pattern of SOD3 expression. In the mouse, *Sod3* mRNA is expressed predominantly in the adrenal gland, kidney, and within type II pneumocytes.²⁴ Focal expression of SOD3 in the lung protects against hyperoxia-induced bronchopulmonary dysplasia as well as bleomycin-induced pulmonary fibrosis.^{25,26} Conversely, knocking out SOD3 worsens lung injury in the bleomycin

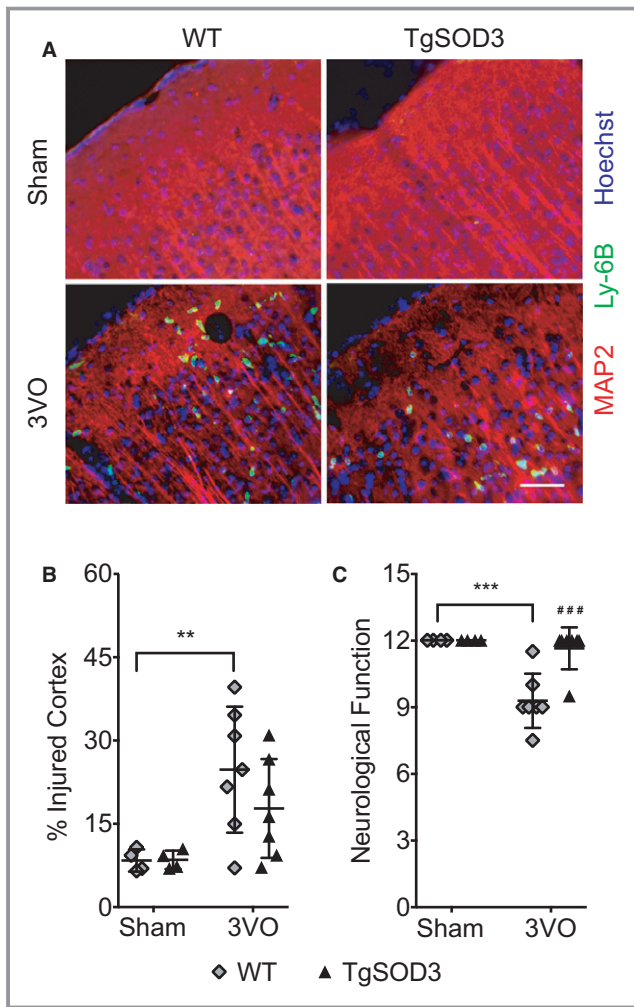


Figure 4. Histologic and functional effects of global cerebral ischemia in wild-type (WT) and TgSOD3 mice. **A**, Immunohistochemical staining of coronal brain sections demonstrate the effects of 3VO on tissue injury, quantified by loss of microtubule-associated protein 2 staining (red), and Ly-6B(+) PMNs (green) transmigration into the cerebral cortex. **B**, Quantification of the extent of 3VO-induced cortical injury graphed as % increase in damaged cortex in post-ischemic relative to sham tissue. **C**, Changes in neurological function score 3 days after treatment. Scale bar=50 μ m. Values represent means \pm SD (n=4–7). Two-way ANOVA with the Holm-Sidak post hoc test: ** P <0.01, *** P <0.001 between sham and 3VO; ### P <0.001 between WT and TgSOD3. 3VO indicates 3-vessel occlusion; PMN, polymorphonuclear neutrophil; TgSOD3, transgenic superoxide dismutase 3.

model.²⁷ Given these findings, we considered whether focal expression of SOD3 in the lung could exert distal, protective effects in the brain. In addition to reducing reactive inflammation in the lung, enhancing SOD3 expression within the lung reduce systemic PMN priming, blood-brain barrier damage, and behavioral changes associated with global cerebral ischemia-reperfusion injury. Our results indicate that endogenous SOD3 may be an important determinant of

cerebrovascular resilience in the setting of central nervous system ischemia-reperfusion injury.

Review of the literature offers several clues regarding the potential mechanism(s) underlying SOD3-dependent protection. Once translated, SOD3 associates with the extracellular matrix, where it reduces the degradation of collagen, hyaluronic acid, and other components that act as damage-associated molecular patterns stimulating local inflammation and immune recruitment.²⁸ SOD3 is also released to the systemic circulation, where it associates with the endothelial glycocalyx.^{18,29,30} The glycocalyx is comprised by a meshlike layer of proteoglycans that provides an important barrier function protecting against leukocyte-endothelial as well as leukocyte-platelet interactions.^{31,32} Thus, in addition to reducing local concentrations of free radicals, SOD3 reduces shedding of the glycocalyx that would otherwise externalize the surface adhesion molecules required for leukocyte transmigration.^{33–35}

The healthy lung exerts an overall anti-inflammatory bias on circulating leukocytes and serves a “catch-and-release” function filtering primed granulocytes out of circulation and exerting a depriving influence as they traverse the pulmonary vasculature.^{13,16,22,36} However, above a critical threshold, it is hypothesized acquired lung injury may short circuit this protective response. For example, using exogenously primed and labeled leukocytes, investigators demonstrated that in acute respiratory distress syndrome PMNs released from the inflamed lung were more activated relative to controls.¹³ In the current study, transient global ischemia was alone sufficient to increase PMN transmigration into the lung. However, while circulating PMNs from TgSOD3/3VO mice expressed lower levels of the leukocyte activation marker CD11b relative to 3VO/WT controls, we found no genotype differences in the cumulative number of PMNs found within the lung or brain. While the catch-and-release model with associated PMN depriving could explain the observed immune effects in our system, further analyses including radiolabeling strategies are required to definitively address this possibility.

SOD3-mediated changes in lung inflammation could also alter the polarization of intraluminal PMNs independent of and prior to tissue transmigration. For example, treatment with the peroxisome proliferator-activated receptor- γ agonist rosiglitazone in a model of focal stroke induced an anti-inflammatory state in PMNs without altering their transmigration into the stroke bed.³⁷ Global SOD3 overexpression induces a similar “N2”-like state in PMNs characterized by lower levels of tumor necrosis factor- α , reduced cytotoxic potential, and propensity to undergo apoptosis.³⁸ While we have not yet confirmed the presence of polarization in our model using markers like YM1 and arginase, our data strongly suggest that in the context of ischemic brain damage, a key

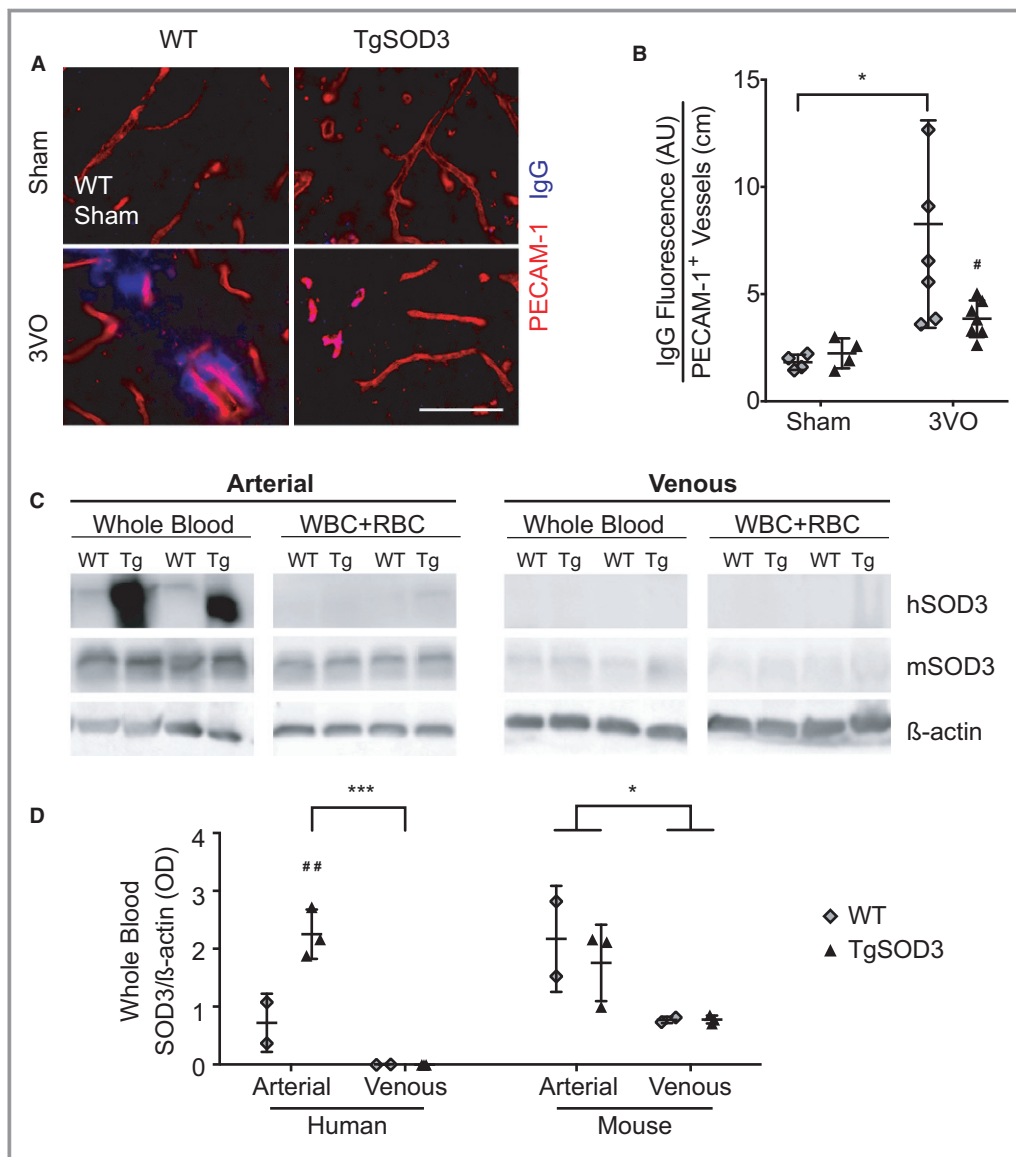


Figure 5. Arterial SOD3 shed from the lung protects against ischemia-induced blood-brain barrier damage. **A**, Micrographs showing PECAM-1(+) vascular endothelial cells (red) and perivascular IgG deposits (blue). Scale bar=50 μ m. **B**, Quantification of immunoglobulin G leakage per vessel length (n=4–7). * P <0.05 between sham and 3VO; # P <0.05 between WT and TgSOD3. **C** and **D**, Localization of SOD3 in circulation. Westerns of hSOD3 and mouse SOD3 levels in arterial vs venous samples and localization within whole blood vs cellular components (WBC+RBC) isolated from naive WT and TgSOD3 mice. Protein levels were normalized to β -actin. Values represent means \pm SD (n=3). Two-way ANOVA with Holm-Sidak post hoc test: * P <0.05, *** P <0.001 between arterial and venous; ## P <0.01 between WT and TgSOD3. hSOD3 indicates human superoxide dismutase 3; mSOD3, mouse superoxide dismutase 3; OD=optical density; PECAM-1, platelet endothelial cell adhesion molecule; RBC, red blood cell; SOD3, superoxide dismutase 3; TgSOD3, transgenic superoxide dismutase 3; WBC, white blood cell; WT, wild type.

function of lung SOD3 is to limit peripheral immune priming initiated by central nervous system damage-associated molecular patterns. That said, it is important to consider that acute brain injury also induces gut dysbiosis and the associated release of bacterial endotoxin.^{39,40} Given studies from our group and others demonstrating the combined

effects of damage-associated molecular pattern and pathogen-associated molecular pattern priming postischemic brain injury,^{9,41} it will be interesting to test whether fluctuations in systemic arterial SOD3 levels exert similar effects on the enteric microvasculature with attendant effects on associated bacterial translocation and endotoxin leak.

The selectivity of the surfactant protein-C promoter and the immunologically distinct human form of SOD3 provided additional insight regarding potential mechanisms leading to neurovascular protection in our model. While SOD3 has been localized to PMN secretory vesicles,⁴² our analyses indicate that the majority of expressed SOD3 was not contained in circulating leukocytes. In addition, both endogenous mouse and human SOD3 protein exhibited an arterial-venous gradient with the highest levels found within the arterial circulation. The magnitude of the SOD3 A-V gradient was also less pronounced for mouse SOD3 as compared with hSOD3, which may relate to the fact that the amino acid sequence for human and mouse SOD3 are only 60% homologous. Although not considered a significant driver of its biological activity, it is intriguing to consider that the sequence diversity present in the glycosylated NH₂-terminus may govern the adhesive properties and varied distribution in vivo.³⁰ Although not directly visualized, our findings are consistent with a gradient of SOD3 deposition across the arterial and capillary beds with relative depletion at the venous phase of circulation. As a corollary to this model, without continuous replenishment of SOD3 in the cerebrovasculature, one might expect to find endothelial injury, microvascular thrombosis, and other features associated with the no-reflow phenomenon elevated in postischemic tissue.⁴³

Conclusions

In the present work, we implicate lung-neurovascular coupling in the pathological response to transient global cerebral ischemia and demonstrate how manipulation of this pathway via targeted expression of hSOD3 in the lung can produce remote cerebrovascular protection.^{20,38} Given its position in the cardiovascular system and importance in postischemic systemic immune priming, these studies also frame the lung as a tractable target for therapeutic intervention. We anticipate that our work will stimulate further exploration regarding the role of lung-neurovascular coupling in related cerebrovascular conditions.

Acknowledgments

The authors thank Min Yee for her technical assistance and Max Sims for technical assistance and formatting of the manuscript.

Author Contributions

Mai, O'Reilly, Kim, and Halterman participated on model development and experimental design. Mai, Miller-Rhodes, and Prifti performed the experiments; and Mai analyzed the data with supervision from Halterman. Mai and Halterman wrote the manuscript with input from Miller-Rhodes, O'Reilly, and Kim.

Sources of Funding

This study was supported by grants from the NINDS (R01-NS092455 to Halterman and F30-NS092168 to Mai) and NIGMS (T32-GM007356 to Mai).

Disclosures

None.

References

- Buck BH, Liebeskind DS, Saver JL, Bang OY, Yun SW, Starkman S, Ali LK, Kim D, Villablanca JP, Salamon N, Razinia T, Ovbiagele B. Early neutrophilia is associated with volume of ischemic tissue in acute stroke. *Stroke*. 2008;39:355–360.
- Yune HY, Chung SP, Park YS, Chung HS, Lee HS, Lee JW, Park JW, You JS, Park I, Lee HS. Delta neutrophil index as a promising prognostic marker in out of hospital cardiac arrest. *PLoS One*. 2015;10:e0120677.
- Maestrini I, Strbian D, Gautier S, Haapaniemi E, Moulin S, Sairanen T, Dequatre-Ponchelle N, Sibolt G, Cordonnier C, Melkas S, Leys D, Tatlisumak T, Bordet R. Higher neutrophil counts before thrombolysis for cerebral ischemia predict worse outcomes. *Neurology*. 2015;85:1408–1416.
- del Zoppo GJ. Acute anti-inflammatory approaches to ischemic stroke. *Ann N Y Acad Sci*. 2010;1207:143–148.
- Furuya K, Takeda H, Azhar S, McCarron RM, Chen Y, Ruetzler CA, Wolcott KM, DeGraba TJ, Rothlein R, Hugli TE, del Zoppo GJ, Hallenbeck JM. Examination of several potential mechanisms for the negative outcome in a clinical stroke trial of enlimomab, a murine anti-human intercellular adhesion molecule-1 antibody: a bedside-to-bench study. *Stroke*. 2001;32:2665–2674.
- Krams M, Lees KR, Hacke W, Grieve AP, Orgogozo JM, Ford GA. Acute stroke therapy by inhibition of neutrophils (astin): an adaptive dose-response study of UK-279,276 in acute ischemic stroke. *Stroke*. 2003;34:2543–2548.
- Samary CS, Ramos AB, Maia LA, Rocha NN, Santos CL, Magalhaes RF, Clevelario AL, Pimentel-Coelho PM, Mendez-Otero R, Cruz FF, Capelozzi VL, Ferreira TPT, Koch T, de Abreu MG, Dos Santos CC, Pelosi P, Silva PL, Rocco PRM. Focal ischemic stroke leads to lung injury and reduces alveolar macrophage phagocytic capability in rats. *Crit Care*. 2018;22:249.
- Toung TJ, Chang Y, Lin J, Bhardwaj A. Increases in lung and brain water following experimental stroke: effect of mannitol and hypertonic saline. *Crit Care Med*. 2005;33:203–208; discussion 259–260.
- Mai N, Prifti L, Rininger A, Bazarian H, Halterman MW. Endotoxemia induces lung-brain coupling and multi-organ injury following cerebral ischemia-reperfusion. *Exp Neurol*. 2017;297:82–91.
- Hogg JC, Doerschuk CM. Leukocyte traffic in the lung. *Annu Rev Physiol*. 1995;57:97–114.
- Andonegui G, Bonder CS, Green F, Mullaly SC, Zbytniuk L, Raharjo E, Kubes P. Endothelium-derived toll-like receptor-4 is the key molecule in LPS-induced neutrophil sequestration into lungs. *J Clin Invest*. 2003;111:1011–1020.
- Woodfin A, Voisin MB, Beyrau M, Colom B, Caille D, Diapouli FM, Nash GB, Chavakis T, Albelda SM, Rainger GE, Meda P, Imhof BA, Nourshargh S. The junctional adhesion molecule jam-c regulates polarized transendothelial migration of neutrophils in vivo. *Nat Immunol*. 2011;12:761–769.
- Summers C, Singh NR, White JF, Mackenzie IM, Johnston A, Solanki C, Balan KK, Peters AM, Chilvers ER. Pulmonary retention of primed neutrophils: a novel protective host response, which is impaired in the acute respiratory distress syndrome. *Thorax*. 2014;69:623–629.
- Kitchen E, Rossi AG, Condliffe AM, Haslett C, Chilvers ER. Demonstration of reversible priming of human neutrophils using platelet-activating factor. *Blood*. 1996;88:4330–4337.
- Singh NR, Johnson A, Peters AM, Babar J, Chilvers ER, Summers C. Acute lung injury results from failure of neutrophil de-priming: a new hypothesis. *Eur J Clin Invest*. 2012;42:1342–1349.
- Nahum A, Chamberlin W, Sznajder JI. Differential activation of mixed venous and arterial neutrophils in patients with sepsis syndrome and acute lung injury. *Am Rev Respir Dis*. 1991;143:1083–1087.
- Marklund SL. Properties of extracellular superoxide dismutase from human lung. *Biochem J*. 1984;220:269–272.
- Ookawara T, Imazeki N, Matsubara O, Kizaki T, Oh-Ishi S, Nakao C, Sato Y, Ohno H. Tissue distribution of immunoreactive mouse extracellular superoxide dismutase. *Am J Physiol*. 1998;275:C840–C847.

19. Zaghoul N, Nasim M, Patel H, Codipilly C, Marambaud P, Dewey S, Schiffer WK, Ahmed M. Overexpression of extracellular superoxide dismutase has a protective role against hyperoxia-induced brain injury in neonatal mice. *FEBS J*. 2012;279:871–881.
20. Zaghoul N, Patel H, Codipilly C, Marambaud P, Dewey S, Frattini S, Huerta PT, Nasim M, Miller EJ, Ahmed M. Overexpression of extracellular superoxide dismutase protects against brain injury induced by chronic hypoxia. *PLoS One*. 2014;9:e108168.
21. Buczynski BW, Mai N, Yee M, Allen JL, Prifti L, Cory-Slechta DA, Halterman MW, O'Reilly MA. Lung-specific extracellular superoxide dismutase improves cognition of adult mice exposed to neonatal hyperoxia. *Front Med*. 2018;5:334.
22. Folz RJ, Abushamaa AM, Suliman HB. Extracellular superoxide dismutase in the airways of transgenic mice reduces inflammation and attenuates lung toxicity following hyperoxia. *J Clin Invest*. 1999;103:1055–1066.
23. Thal SC, Thal SE, Plesnila N. Characterization of a 3-vessel occlusion model for the induction of complete global cerebral ischemia in mice. *J Neurosci Methods*. 2010;192:219–227.
24. Yue F, Cheng Y, Breschi A, Vierstra J, Wu W, Ryba T, Sandstrom R, Ma Z, Davis C, Pope BD, Shen Y, Pervouchine DD, Djebali S, Thurman RE, Kaul R, Rynes E, Kirilusha A, Marinov GK, Williams BA, Trout D, Amrhein H, Fisher-Aylor K, Antoshechkin I, DeSalvo G, See LH, Fastuca M, Drenkow J, Zaleski C, Dobin A, Prieto P, Lagarde J, Bussotti G, Tanzer A, Denas O, Li K, Bender MA, Zhang M, Byron R, Groudine MT, McCleary D, Pham L, Ye Z, Kuan S, Edsall L, Wu YC, Rasmussen MD, Bansal MS, Kellis M, Keller CA, Morrissey CS, Mishra T, Jain D, Dogan N, Harris RS, Cayting P, Kawli T, Boyle AP, Euskirchen G, Kundaje A, Lin S, Lin Y, Jansen C, Malladi VS, Cline MS, Erickson DT, Kirkup VM, Learned K, Sloan CA, Rosenbloom KR, Lacerda de Sousa B, Beal K, Pignatelli M, Flicek P, Lian J, Kahveci T, Lee D, Kent WJ, Ramalho Santos M, Herrero J, Notredame C, Johnson A, Vong S, Lee K, Bates D, Neri F, Diegel M, Canfield T, Sabo PJ, Wilken MS, Reh TA, Giste E, Shafer A, Kutayin T, Haugen E, Dunn D, Reynolds AP, Neph S, Humbert R, Hansen RS, De Bruijn M, Selleri L, Rudensky A, Josefowicz S, Samstein R, Eichler EE, Orkin SH, Levasseur D, Papayannopoulou T, Chang KH, Skoultschi A, Gosh S, Disteche C, Treuting P, Wang Y, Weiss MJ, Blobel GA, Cao X, Zhong S, Wang T, Good PJ, Lowdon RF, Adams LB, Zhou XQ, Pazin MJ, Feingold EA, Wold B, Taylor J, Mortazavi A, Weissman SM, Stamatoyannopoulos JA, Snyder MP, Guigo R, Gingeras TR, Gilbert DM, Hardison RC, Beer MA, Ren B, Mouse EC. A comparative encyclopedia of DNA elements in the mouse genome. *Nature*. 2014;515:355–364.
25. Buczynski BW, Yee M, Martin KC, Lawrence BP, O'Reilly MA. Neonatal hyperoxia alters the host response to influenza a virus infection in adult mice through multiple pathways. *Am J Physiol Lung Cell Mol Physiol*. 2013;305:L282–L290.
26. Van Rheen Z, Fattman C, Domarski S, Majka S, Klemm D, Stenmark KR, Nozik-Grayck E. Lung extracellular superoxide dismutase overexpression lessens bleomycin-induced pulmonary hypertension and vascular remodeling. *Am J Respir Cell Mol Biol*. 2011;44:500–508.
27. Delaney C, Wright RH, Tang JR, Woods C, Villegas L, Sherlock L, Savani RC, Abman SH, Nozik-Grayck E. Lack of EC-SOD worsens alveolar and vascular development in a neonatal mouse model of bleomycin-induced bronchopulmonary dysplasia and pulmonary hypertension. *Pediatr Res*. 2015;78:634–640.
28. Nozik-Grayck E, Suliman HB, Piantadosi CA. Extracellular superoxide dismutase. *Int J Biochem Cell Biol*. 2005;37:2466–2471.
29. Oury TD, Day BJ, Crapo JD. Extracellular superoxide dismutase in vessels and airways of humans and baboons. *Free Radic Biol Med*. 1996;20:957–965.
30. Folz RJ, Guan J, Seldin MF, Oury TD, Enghild JJ, Crapo JD. Mouse extracellular superoxide dismutase: primary structure, tissue-specific gene expression, chromosomal localization, and lung in situ hybridization. *Am J Respir Cell Mol Biol*. 1997;17:393–403.
31. Reitsma S, Slaaf DW, Vink H, van Zandvoort MA, oude Egbrink MG. The endothelial glycocalyx: composition, functions, and visualization. *Pflugers Arch*. 2007;454:345–359.
32. Renesto P, Si Tahar M, Chignard M. Modulation by superoxide anions of neutrophil-mediated platelet activation. *Biochem Pharmacol*. 1994;47:1401–1404.
33. Bonder CS, Knight D, Hernandez-Saavedra D, McCord JM, Kubes P. Chimeric SOD2/3 inhibits at the endothelial-neutrophil interface to limit vascular dysfunction in ischemia-reperfusion. *Am J Physiol Gastrointest Liver Physiol*. 2004;287:G676–G684.
34. Laurila JP, Laatikainen LE, Castellone MD, Laukkanen MO. SOD3 reduces inflammatory cell migration by regulating adhesion molecule and cytokine expression. *PLoS One*. 2009;4:e5786.
35. Shuvaev VV, Han J, Yu KJ, Huang S, Hawkins BJ, Madesh M, Nakada M, Muzykantov VR. Pecam-targeted delivery of SOD inhibits endothelial inflammatory response. *FASEB J*. 2011;25:348–357.
36. Tam FW, Clague J, Dixon CM, Stuttle AW, Henderson BL, Peters AM, Lavender JP, Ind PW. Inhaled platelet-activating factor causes pulmonary neutrophil sequestration in normal humans. *Am Rev Respir Dis*. 1992;146:1003–1008.
37. Cuartero MI, Ballesteros I, Moraga A, Nombela F, Vivancos J, Hamilton JA, Corbi AL, Lizasoain I, Moro MA. N2 neutrophils, novel players in brain inflammation after stroke: modulation by the PPARgamma agonist rosiglitazone. *Stroke*. 2013;44:3498–3508.
38. Break TJ, Jun S, Indramohan M, Carr KD, Sieve AN, Dory L, Berg RE. Extracellular superoxide dismutase inhibits innate immune responses and clearance of an intracellular bacterial infection. *J Immunol*. 2012;188:3342–3350.
39. Grimaldi D, Sauneuf B, Guivarch E, Ricome S, Geri G, Charpentier J, Zuber B, Dumas F, Spaulding C, Mira JP, Cariou A. High level of endotoxemia following out-of-hospital cardiac arrest is associated with severity and duration of postcardiac arrest shock. *Crit Care Med*. 2015;43:2597–2604.
40. Klimiec E, Pera J, Chrzanowska-Wasko J, Golenia A, Slowik A, Dziedzic T. Plasma endotoxin activity rises during ischemic stroke and is associated with worse short-term outcome. *J Neuroimmunol*. 2016;297:76–80.
41. Denes A, McColl BW, Leow-Dyke SF, Chapman KZ, Humphreys NE, Grecnis RK, Allan SM, Rothwell NJ. Experimental stroke-induced changes in the bone marrow reveal complex regulation of leukocyte responses. *J Cereb Blood Flow Metab*. 2011;31:1036–1050.
42. Iversen MB, Gottfredsen RH, Larsen UG, Enghild JJ, Praetorius J, Borregaard N, Petersen SV. Extracellular superoxide dismutase is present in secretory vesicles of human neutrophils and released upon stimulation. *Free Radic Biol Med*. 2016;97:478–488.
43. Rezkalla SH, Kloner RA. No-reflow phenomenon. *Circulation*. 2002;105:656–662.